Electronic Supplementary Material (ESI) for Chemical Communications

P-P Menschutkin preparation of prototypical phosphinophosphonium salts

Saurabh S. Chitnis,[§] Elizabeth MacDonald,[#] Neil Burford,[§#] Ulrike Werner-Zwanziger[#] and Robert McDonald†*

[§]Department of Chemistry, University of Victoria, Victoria BC, V8W 3V6, Canada

Email: nburford@uvic.ca

[#]Department of Chemistry, Dalhousie University, Halifax, NS, B3H 4J3, Canada

[†]X-ray Crystallography Laboratory, Department of Chemistry, University of Alberta, Edmonton, Alberta T6G 2G2, Canada

Supporting Information

Experimental

General: Reactions were carried out in an MBraun Labmaster 130 glovebox under an atmosphere of dry N_2. CH_2Cl_2 and pentane were purified on an MBraun solvent purification system and stored over 4 Å molecular sieves. MeCN and fluorobenzene were purchased from Aldrich, distilled from CaH_2 under an atmosphere of argon and stored over 4 Å molecular sieves. Deuterated solvents were purchased from Aldrich and dried using 4 Å molecular sieves. The phosphines PMe_3, PPh_3, Me_2PCl, $MePCl_2$, PhP_2PCl, $PhPCl_2$ and PCl_3 were obtained from Aldrich and used as received. $Me_3SiOSO_2CF_3$ was purchased from Aldrich and distilled prior to use.

Solution state ^{31}P NMR spectra were obtained at room temperature, unless otherwise stated, on a Bruker AVANCE 300 ^{1}H (300.15 MHz, 7.02 T). Chemical shifts (δ) are reported in ppm. ^{13}C (125.76 MHz) chemical shifts are referenced to δ_{TMS} = 0.00 ppm, ^{31}P (202.46 MHz, 121.56 MHz) chemical shifts are referenced to $\delta_{H3PO4\ (85\%)}$ = 0.00 ppm. Solution-phase spectra were obtained on aliquots of reaction mixtures in appropriate deuterated solvent in a 5 mm tube. The tubes were capped and sealed with Teflon and Parafilm prior to removal from the inert atmosphere. Solid-phase spectra were obtained on dried powders obtained after removal of solvent under vacuum. The powders were loaded into sample holders inside the glovebox. Solid state ^{31}P cross-polarization (CP) / magic angle spinning (MAS) NMR spectra were acquired on a Bruker DSX NMR spectrometer operating at 9.4T (400.24 MHZ ^{1}H, 162.02MHz ^{31}P Larmor frequencies) using rotors of 4mm diameter and 2.5mm diameters. Spinning speeds were varied up to 12 kHz and up to 23 kHz for the 4mm and 2.5mm rotors, respectively, to identify the isotropic shifts and spinning sidebands. Using CP contact times of 500 μs, up to 80 scans were accumulated with repetition times of up to 5s. The chemical shift scale was referenced externally against $NH_4H_2PO_4$ at 0.81ppm as secondary standard.

Raman spectra were obtained in sealed capillaries under N_2 at room temperature. Peaks are reported in wavenumbers (cm^{-1}) with ranked intensities in parentheses, where a value of 100 is indicative of the most intense peak in the spectrum. Melting points were recorded on an Electrothermal apparatus in sealed capillary tubes under N_2. Elemental analyses of selected samples were performed by Canadian Microanalytical Services Ltd. Delta, British Columbia, Canada.

A*b initio* calculations were performed using Gaussian09.[1] All structures were optimized without symmetry constraints at the MP2 level using the frozen-core approximation and Dunning's cc-pVTZ basis-set.[2] All structures were verified as true minima by noting the absence of any imaginary frequencies. The composite G3B3 method[3] was used to compute standard enthalpies at 298K. Basis-set superposition errors were treated using Counterpoise correction.[4]

Synthesis and characterization of $[Me_3PPMe_2][Cl]$, (**3**)[Cl]

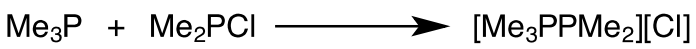

Me_2PCl (0.483 g, 5 mmol) was added to a glass bulb equipped with a teflon stir bar and frozen at −196°C. Me_3P (0.381 g, 5 mmol) was condensed and frozen onto the walls of the bulb at −196°C and any non-condensed material was removed under dynamic vacuum. The bulb was allowed to warm to room temperature with stirring for 5 minutes to yield a fine white powder, which was subjected to dynamic vacuum for 6 hours to remove any volatiles (crude yield = 0.859 g, 99%). A portion of the crude powder was removed for solid-state NMR analysis and the remainder (0.349 g) was sublimed under dynamic vacuum at approximately 70°C to yield the title product as a fine white powder (0.276 g, 77%). Due to the low solubility of the powder, a high-resolution solution NMR could not be obtained. For the same reason only a small amount of crystals (< 2 % yield) were isolated from a saturated CH_3CN solution over 1 week at −30°C and identified as $[Me_3PPMe_2][Cl]$ using X-ray crystallography. The sublimation range and the elemental composition of the crystals are identical to those of the bulk powder.

Yield (fractional yield of sublimation extended to bulk): 0.661 g (77%);

Melting Point: 190-197°C sublimes;

Elemental Analysis (calc.) Found [Δ]: C (34.80) 34.54[0.26], H (8.76) 8.15[0.61];

Raman (Int.): 83.9 (16), 245.2 (33), 259.9 (15), 268.4 (27), 280.6 (12), 292.8 (9), 329.5 (15), 449.2 (66) = $\nu_{P\text{-}P}$, 537.2 (14), 666.7 (32), 672.8 (12), 691.1 (72), 713.1 (30), 774.2 (25), 1391.1 (15), 1416.7 (8), 1433.6 (29), 1460.7 (27), 2082.5 (10), 2474.7 (12), 2800.9 (8), 2808.2 (8), 2830.2 (11), 2858.3 (55), 2865.6 (32), 2879.0 (32), 2897. 4 (96), 2914.5 (45), 2948.7 (91), 2957.2 (92), 2964.6 (100), 2980.4 (43), 3001.2 (31);

^{31}P SS-NMR(12 kHz): -65.9 (d, 242 Hz), 20.0 (d, 256 Hz). Spinning sidebands are indicated by *, by products by †.

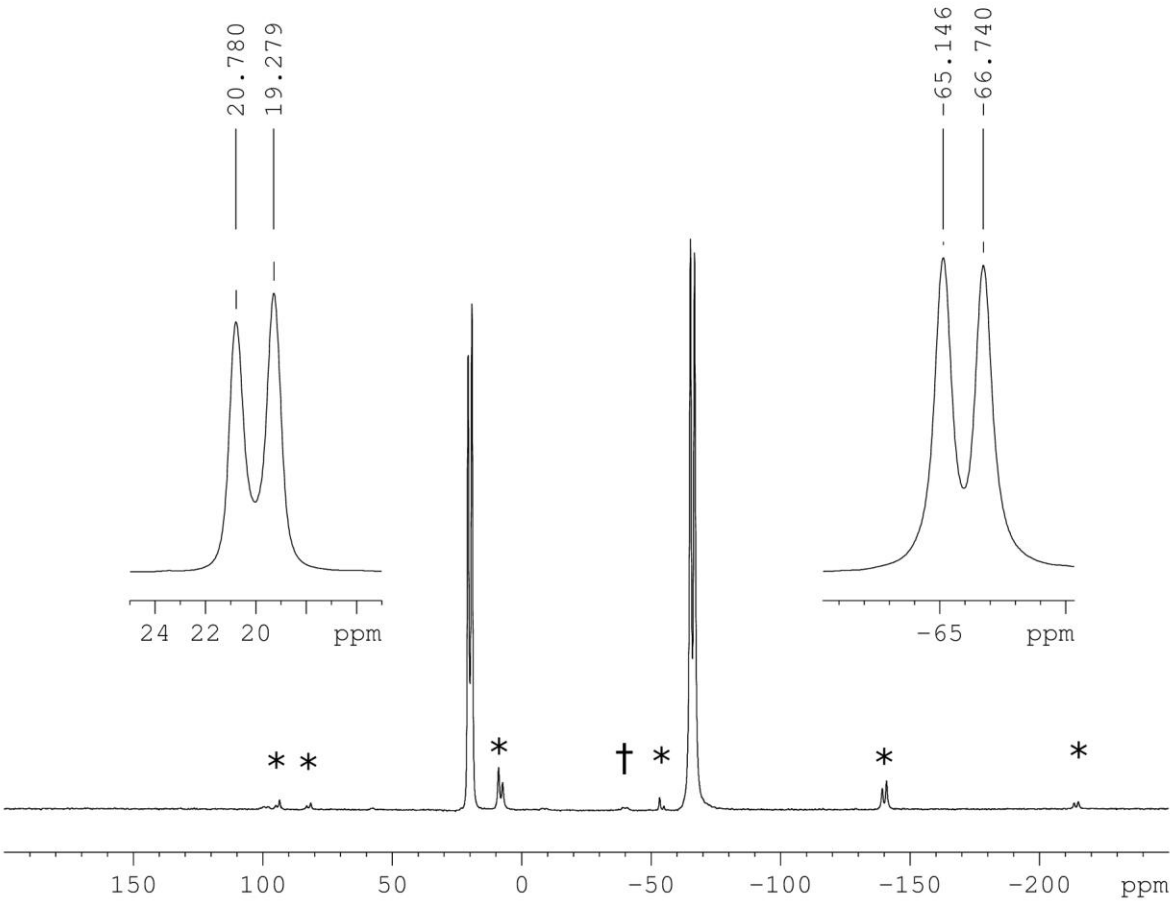

Fig. S1. P-31 CP/MAS spectrum of (**3**)[Cl].

Table S1. Crystallographic Experimental details for (**3**)[Cl].

A. Crystal Data	
formula	$C_5H_{15}ClP_2$
formula weight	172.56
crystal dimensions (mm)	0.39 × 0.11 × 0.10
crystal system	orthorhombic
space group	$Pmn2_1$ (No. 31)
unit cell parameters[a]	
a (Å)	9.4581 (6)
b (Å)	6.5601 (4)
c (Å)	7.3060 (5)
V (Å^3)	453.31 (5)
Z	2
ρ_{calcd} (g cm^{-3})	1.264
μ (mm^{-1})	0.690

B. Data Collection and Refinement Conditions

diffractometer	Bruker D8/APEX II CCD[b]
radiation (λ [Å])	graphite-monochromated Mo Kα (0.71073)
temperature (°C)	–100
scan type	ω scans (0.3°) (15 s exposures)
data collection 2θ limit (deg)	55.02
total data collected	3886 ($-12 \le h \le 12$, $-8 \le k \le 8$, $-9 \le l \le 9$)
independent reflections	1106 (R_{int} = 0.0167)
number of observed reflections (*NO*)	1083 [$F_o^2 \ge 2\sigma(F_o^2)$]
structure solution method	direct methods (*SHELXS–97*[c])
refinement method	full-matrix least-squares on F^2 (*SHELXL–97*[c])
absorption correction method	Gaussian integration (face-indexed)
range of transmission factors	0.9317–0.7760
data/restraints/parameters	1106 / 0 / 48
Flack absolute structure parameter[d]	0.19(8)
goodness-of-fit (*S*)[e] [all data]	1.110
final *R* indices[f]	
R_1 [$F_o^2 \ge 2\sigma(F_o^2)$]	0.0177
wR_2 [all data]	0.0465
largest difference peak and hole	0.239 and –0.189 e Å^{-3}

[a]Obtained from least-squares refinement of 3338 reflections with $7.04° < 2\theta < 54.78°$.

[b]Programs for diffractometer operation, data collection, data reduction and absorption correction were those supplied by Bruker.

[c]Sheldrick, G. M. *Acta Crystallogr.* **2008**, *A64*, 112–122.

[d]Flack, H. D. *Acta Crystallogr.* **1983**, *A39*, 876–881; Flack, H. D.; Bernardinelli, G. *Acta Crystallogr.* **1999**, *A55*, 908–915; Flack, H. D.; Bernardinelli, G. *J. Appl. Cryst.* **2000**, *33*, 1143–1148. The Flack parameter will refine to a value near zero if the structure is in the correct configuration and will refine to a value near one for the inverted configuration. The value observed herein is indicative of a moderate degree of racemic twinning, and was accommodated during the refinement (using the *SHELXL-97* TWIN instruction [see reference *c*]).

[e]$S = [\Sigma w(F_o^2 - F_c^2)^2/(n-p)]^{1/2}$ (n = number of data; p = number of parameters varied; $w = [\sigma^2(F_o^2) + (0.0265P)^2 + 0.0418P]^{-1}$ where $P = [\mathrm{Max}(F_o^2, 0) + 2F_c^2]/3$).

[f]$R_1 = \Sigma||F_o| - |F_c||/\Sigma|F_o|$; $wR_2 = [\Sigma w(F_o^2 - F_c^2)^2/\Sigma w(F_o^4)]^{1/2}$.

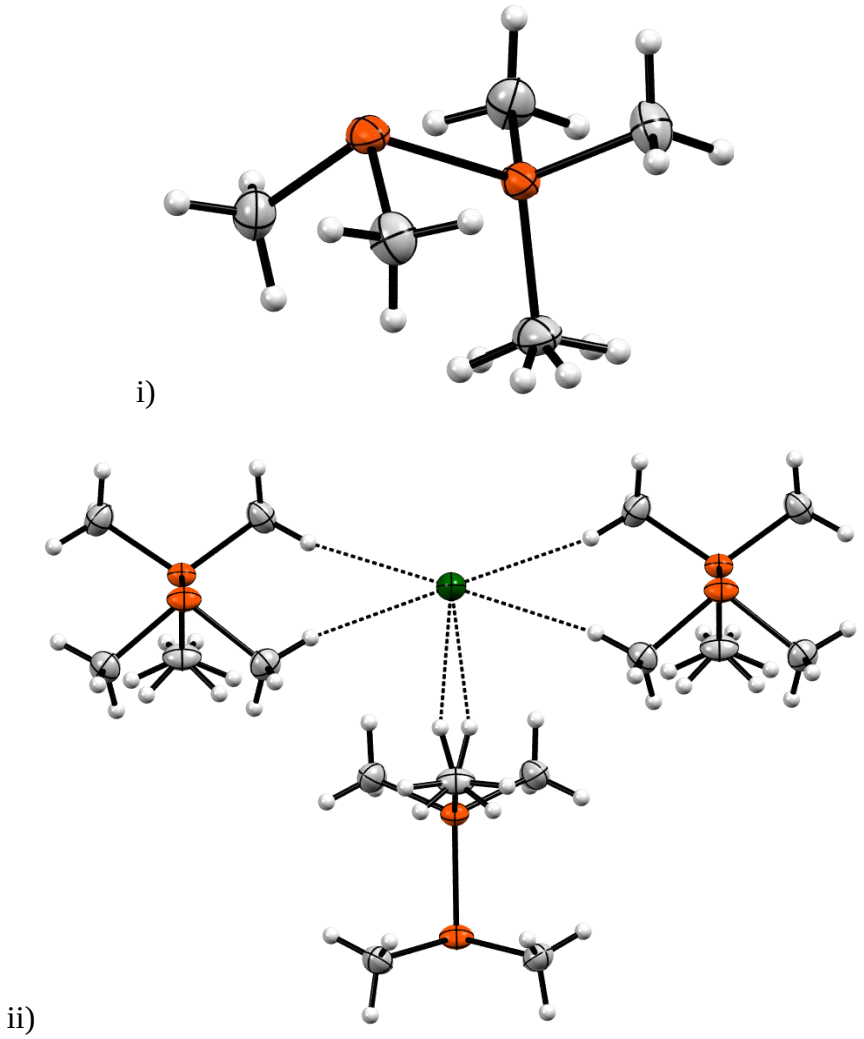

Fig S2. POV-Ray views of i) the cation $[Me_3PPMe_2]^+$ and, ii) Cl---H contacts in $[Me_3PPMe_2][Cl]$.

NMR detection of $[(Me_3P)_2PMe][Cl]_2$, (**4**)$[Cl]_2$

$MePCl_2$ (0.059 mg, 0.5 mmol) and Me_3P (0.076 g, 1 mmol) were combined in 2 mL CD_3CN and stirred for 5 minutes to yield a white suspension. The solvent was removed under dynamic vacuum and white powder, obtained in essentially quantitative yield, was characterized using P-31 CPMAS NMR.

Melting Point: 205-220°C sublimes;

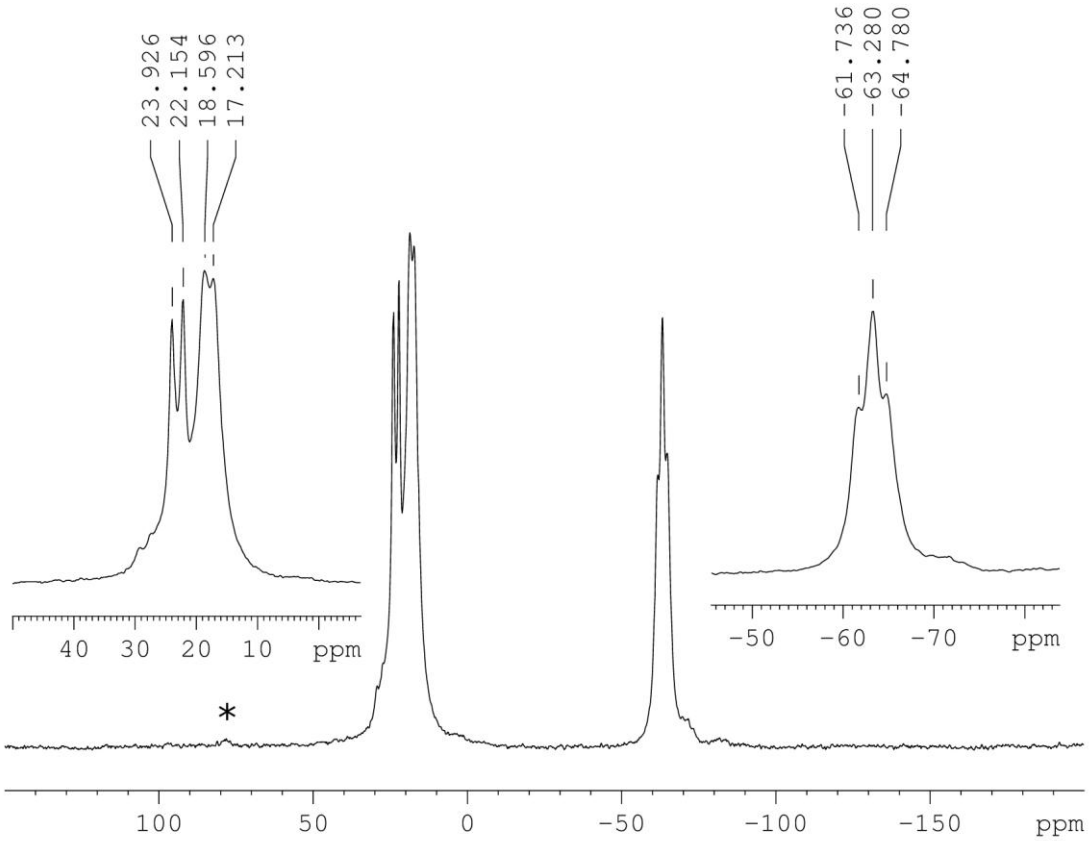

Fig. S3. P-31 CP/MAS spectrum of (**4**)$[Cl]_2$.

Synthesis and characterization of [dmpe(PMe$_2$)$_2$][Cl]$_2$, (5)[Cl]$_2$

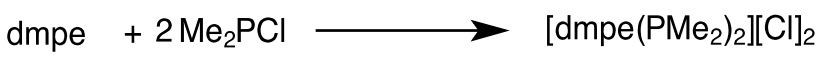

Me_2PCl (0.291 g, 3 mmol) was added to a glass bulb equipped with a Teflon stir bar and frozen at −196°C. Dmpe (0.450 g, 3 mmol) was condensed and frozen onto the walls of the bulb at −196°C and any non-condensed material was removed under dynamic vacuum. The bulb was allowed to warm to room temperature with stirring for 5 minutes to yield a fine white powder, which was subjected to dynamic vacuum for 12 hours to remove any volatiles (crude yield = 0.487 g, 95%). A portion of the crude powder was removed for solid-state NMR analysis and the remained (0.113 g) was sealed in a glass tube and sublimed under static vacuum at 80°C to yield a fine white powder (0.106 g, 94%). Repeated attempts to grow crystals from a saturated CH_3CN solution failed to produce crystalline material. Approximately 0.040 g of the sublimed material was sealed in a glass tube under static vacuum and placed vertically in an oven at 80°C with one end of the tube touching the heating element and the other free of any contact.

Yield (fractional yield of sublimation extended to bulk): 0.458 g, 94%;

Melting point: 185-200°C sublimes;

Elemental Analysis (calc.) Found [Δ]: C (35.00) 34.68[0.32], H (8.22) 7.78[0.44];

^{31}P SS-NMR (12 kHz): -75.1 (*d*, 273 Hz), 29.5 (*d*, 271 Hz). Spinning sidebands are indicated by *.

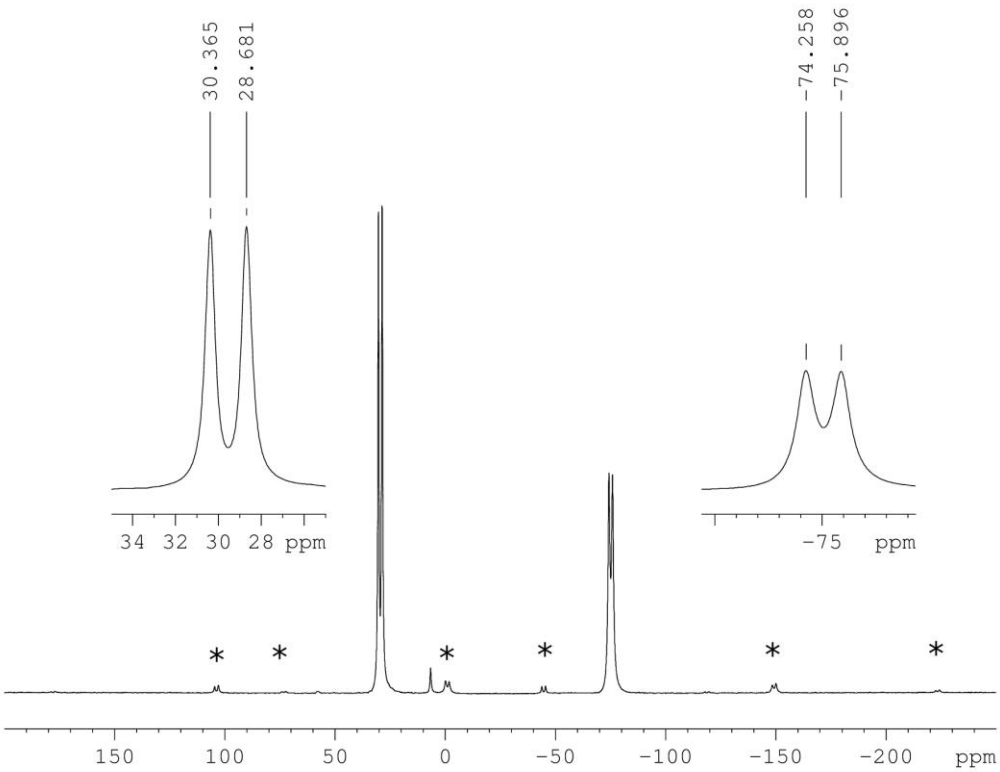

Fig. S4. P-31 CP/MAS spectrum of (**5**)[Cl]$_2$.

NMR detection of [dmpe(PMe$_2$)$_2$][OTf]$_2$, (5)[OTf]$_2$

Me_2PCl (0.096 g, 1 mmol) was combined with TMSOTf (0.222 g, 1 mmol) and stirred for 20 minutes in CD_3CN. A solution of dmpe (0.075 g, 0.5 mmol) in CD_3CN was added and the resulting white suspension was allowed to stir for 20 minutes. The clear and colourless supernatant was analyzed using solution NMR spectroscopy. The ^{31}P NMR and ^{1}H NMR spectra of the supernatant matched that of the precipitate dissolved in fresh CD_3CN.

$^{31}P\{1H\}$ NMR (CD_3CN, 120 MHz, 298 K): -58 (broad, *d*), 23.8 (broad, *d*)

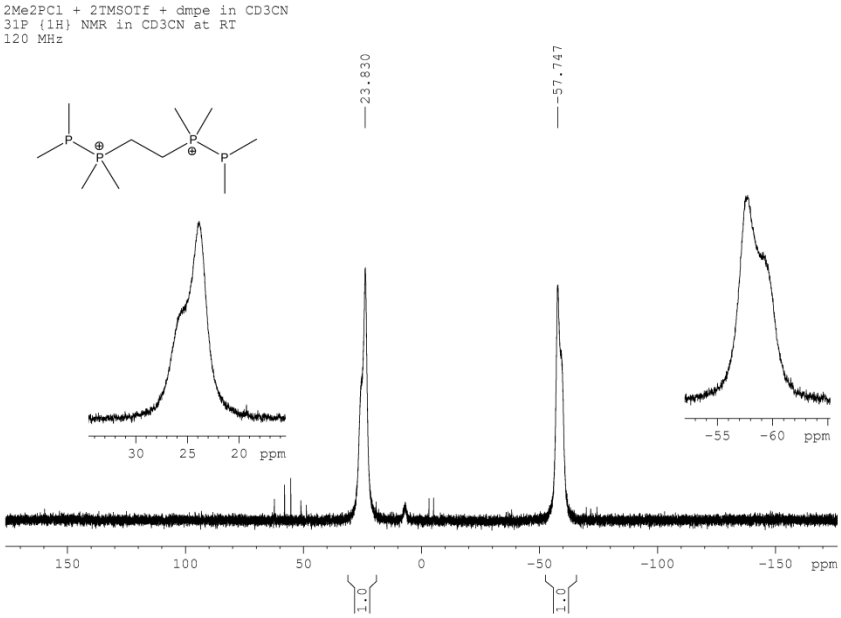

Fig. S5. $^{31}P\{^{1}H\}$ NMR spectrum of (**5**)[OTf]$_2$ in CD_3CN.

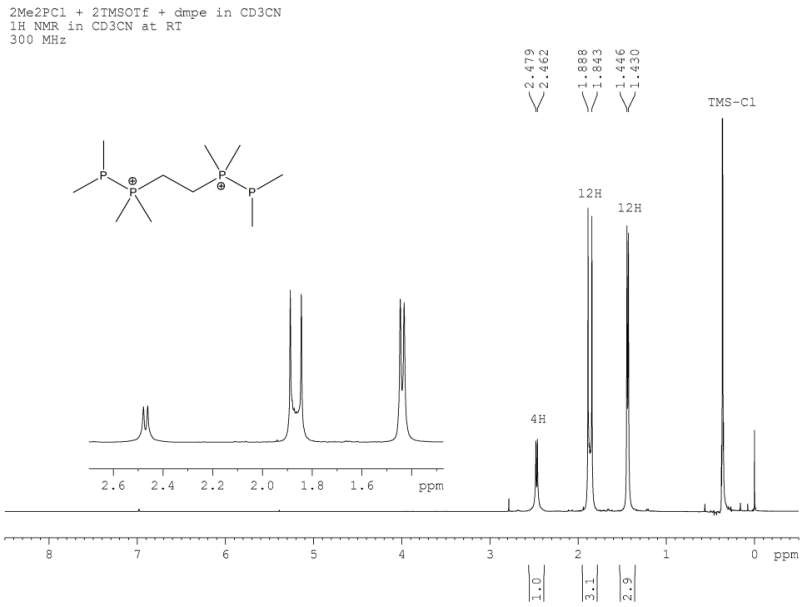

Fig. S6. ^{1}H NMR spectrum of (**5**)[OTf]$_2$ in CD_3CN.

Synthesis and characterization of [dmpePMe][Cl]$_2$, (6)[Cl]$_2$

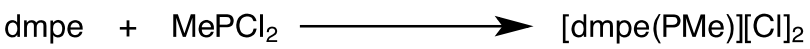

$MePCl_2$ (0.148 g, 1.27 mmol) in 3 mL CH_2Cl_2 was added to a glass bulb equipped with a Teflon stir bar and cooled to −30°C. Dmpe (0.191 g, 1.27 mmol) was dissolved in CH_2Cl_2 and added at once to the stirring solution to immediately yield a large amount of white precipitate. The suspension was stirred for an additional 5 minutes and then placed under vacuum to remove all volatiles to yield a fine white powder (crude yield = 0.330 g, 97%). The powder was washed with 5 mL CH_3CN and placed under dynamic vacuum for 12 hours to remove any volatiles. The resulting fluffy white powder (0.317 g), which is difficult to handle as it easily develops static charge, was found to be analytically pure.

Yield: 0.227 g, 94 %

Melting Point: 197-205°C sublimes;

Elemental Analysis (calcd.) Found [Δ]: C (31.48) 31.25[0.23] H (7.17) 7.17[0.00]

^{31}P SS-NMR (9 kHz): -86.4 (*t*, 271 Hz), 49.8 (*dd*, 296 Hz). Spinning sidebands are indicated by *.

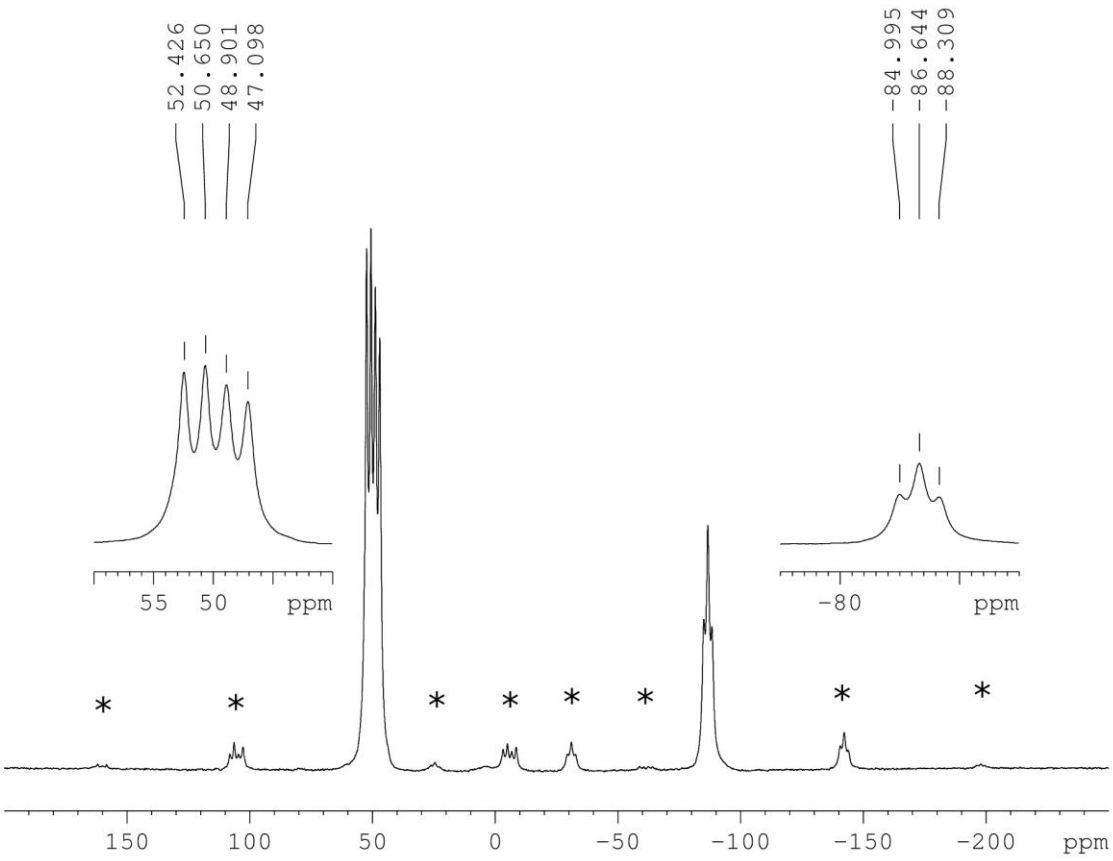

Fig. S7. P-31 CP/MAS spectrum of (**6**)[Cl]$_2$.

NMR detection of [dmpePMe][OTf]$_2$, (6)[OTf]$_2$

$MePCl_2$ (0.058 mg, 0.5 mmol) and TMSOTf (0.222 mg, 1 mmol) were combined in 1 mL CD_3CN and stirred for 5 minutes. A solution of dmpe (0.075 mg, 0.5 mmol) in CD_3CN (1 mL) was added and the reaction mixture was stirred for 5 minutes to yield a clear and colourless supernatant above a small amount of white precipitate. The ^{31}P NMR of the supernatant matched that of the precipitate dissolved in fresh CD_3CN.

$^{31}P\{1H\}$ NMR (CD_3CN, 122 MHz, 298 K): -88.1 (*dd*, $^1J_{P\text{-}P}$ = 278 Hz, $^1J_{P\text{-}P'}$ = 283 Hz), 53.4 (*d*, $^1J_{P\text{-}P}$ = 281 Hz)

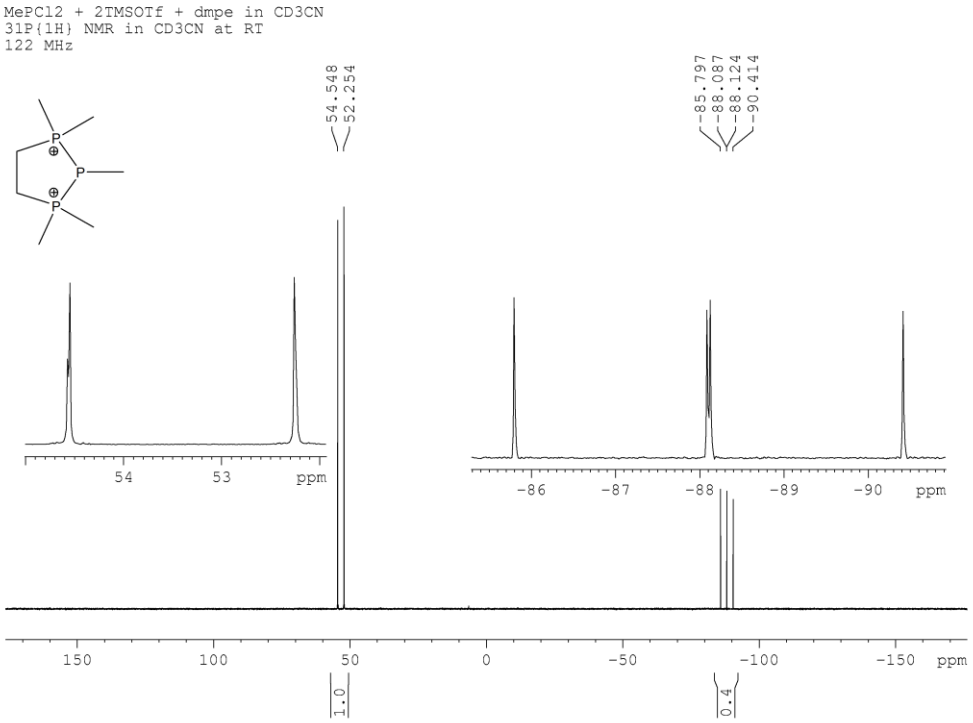

Fig. S8. $^{31}P\{^1H\}$ NMR spectrum of (**6**)[OTf]$_2$ in CD_3CN.

NMR detection of $[Me_3PPPh_2][Cl]_2$, (7)$[Cl]_2$

Ph_2PCl (0.110 mg, 0.5 mmol) and PMe_3 (0.035 mg, 0.5 mmol) were combined in CD_3CN (2 mL) and the reaction mixture was stirred for 5 minutes to yield a clear and colourless solution. The crude reaction mixture was analyzed using ^{31}P and ^{1}H NMR spectroscopy.

$^{31}P\{1H\}$ NMR (CD_3CN, 122 MHz, 298 K): -24 (*s*, broad), 15 (*s*, broad)

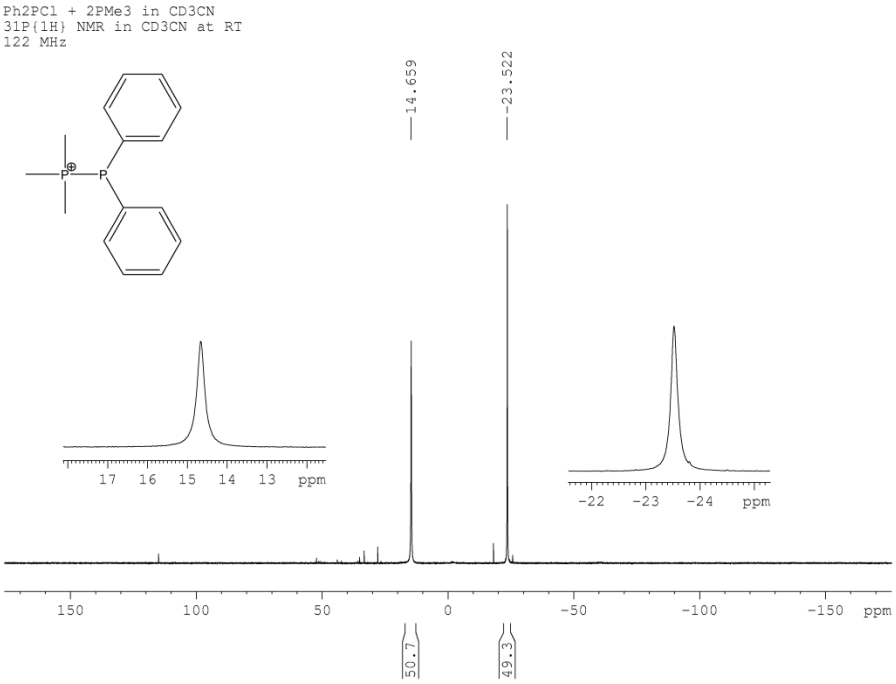

Fig. S9. $^{31}P\{^{1}H\}$ NMR spectrum of (**7**)$[Cl]_2$ in CD_3CN.

NMR detection of $[(Me_3P)_2PPh][Cl]_2$, (8)$[Cl]_2$

$PhPCl_2$ (0.089 mg, 0.5 mmol) and Me_3P (0.076 g, 1 mmol) were combined in 2 mL CD_3CN and stirred for 5 minutes to yield a white suspension. The solvent was removed under vacuum and solids characterized using P-31 CPMAS NMR, melting point and elemental analysis.

Melting Point: 215-225°C sublimes;

Elemental Analysis (calcd.) Found [Δ]: C (43.53) 43.13[0.40] H (6.32) 7.17[0.85]
Note: exposure to dynamic vacuum in preparation for elemental analysis led to decomposition, giving a sticky white solid.

^{31}P SS NMR (11 kHz): 96 (*s*, broad, Me_3PCl_2), 33 (*s*, broad), 30 (*s*, broad), 2 (*s*, broad), -51 (*s*, very broad). Spinning sidebands are indicated by *.

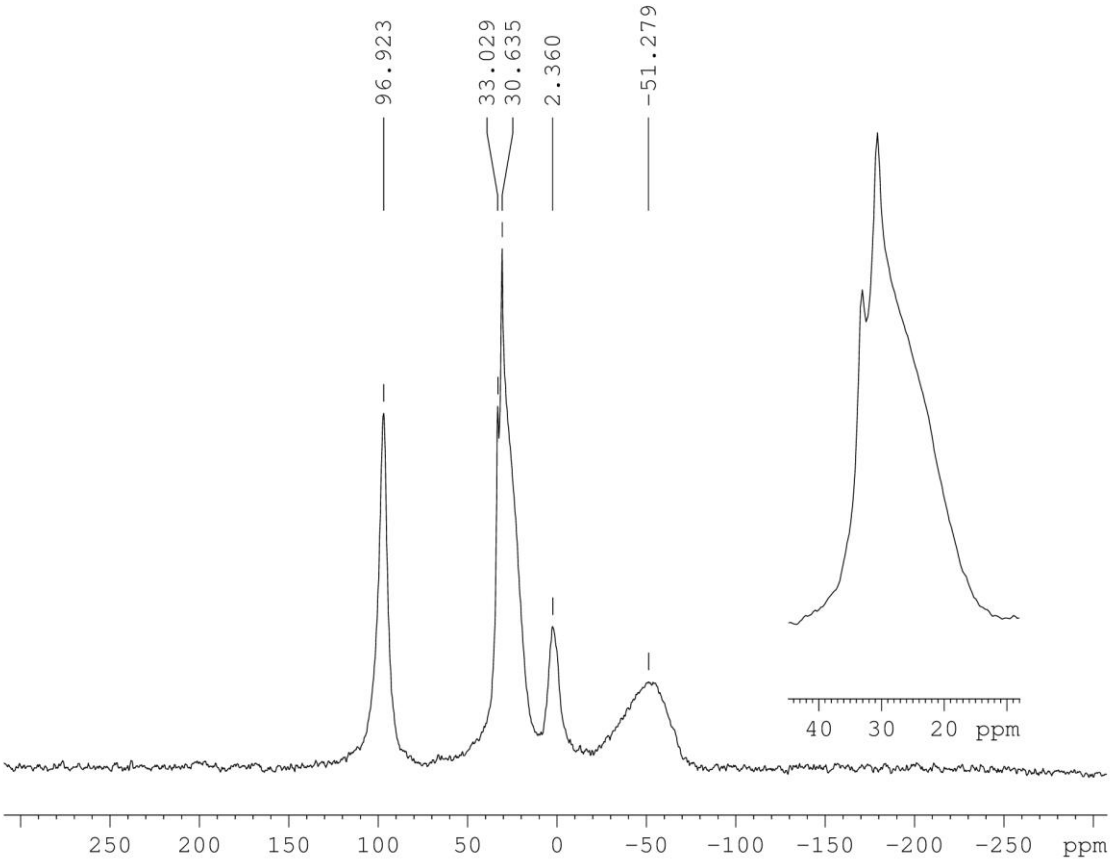

Fig. S10. P-31 CP/MAS spectrum of (**8**)$[Cl]_2$ showing signals due to decomposition products: Me_3PCl_2 and *cyclo*-P_4Ph_4.

NMR detection of [dmpe(PPh$_2$)$_2$][Cl]$_2$, (9)[Cl]$_2$

Ph_2PCl (0.220 mg, 1 mmol) and dmpe (0.075 g, 0.5 mmol) were combined in 2 mL CD_2Cl_2 and stirred for 5 minutes to yield a clear, light pink solution. The crude reaction mixture was analyzed using ^{31}P and ^{1}H NMR spectroscopy.

$^{31}P\{1H\}$ NMR (CD_3CN, 122 MHz, 298 K): -13 (*s*, broad), 20 (*s*, broad)

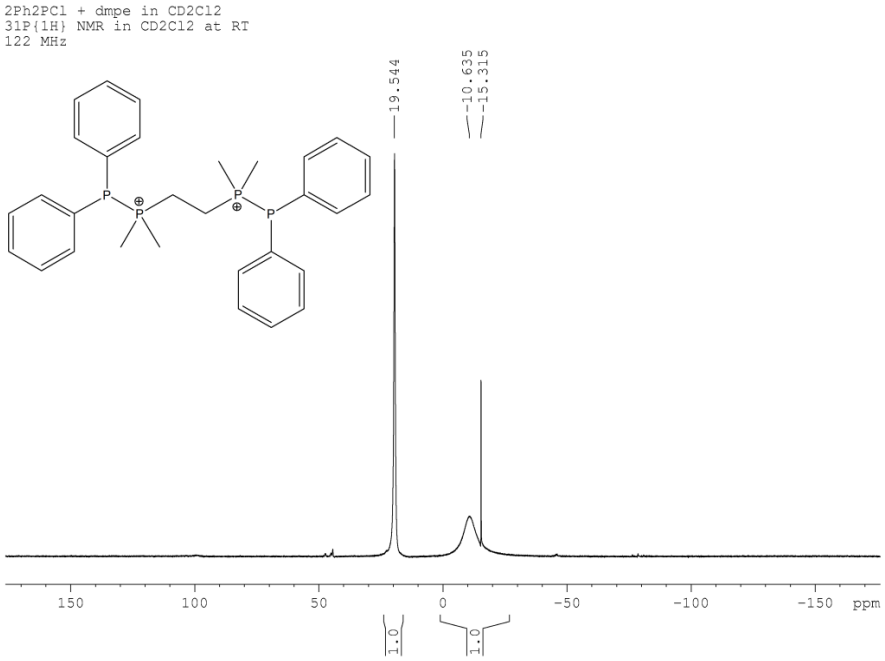

Fig. S11. $^{31}P\{^{1}H\}$ NMR spectrum of (**7**)[Cl]$_2$ in CD_2Cl_2.

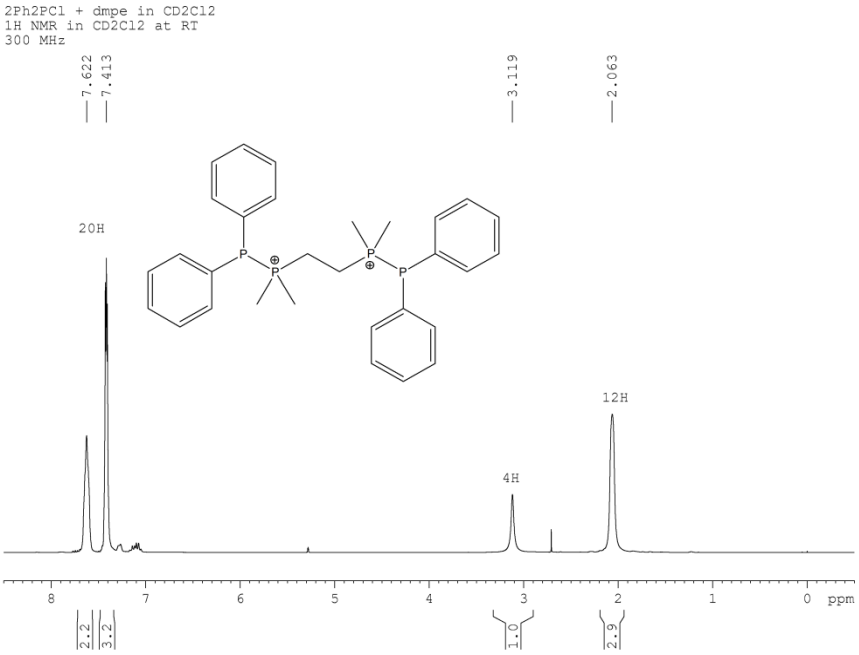

Fig. S12. ^{1}H NMR spectrum of (**7**)[Cl]$_2$ in CD_2Cl_2.

NMR detection of [dmePPh][Cl]$_2$, (10**)[Cl]$_2$**

$PhPCl_2$ (0.180 mg, 1 mmol) and dmpe (0.150 g, 1 mmol) were combined in 2 mL CH_3CN and stirred for 5 minutes to yield a white suspension. The solvent was removed under dynamic vacuum and solids characterized using P-31 CPMAS NMR.

Melting Point: 176-193°C sublimes;

^{31}P SS NMR (8 kHz): 48 (*s*, broad), -77 (*s*, broad). Spinning side bands are indicated by *

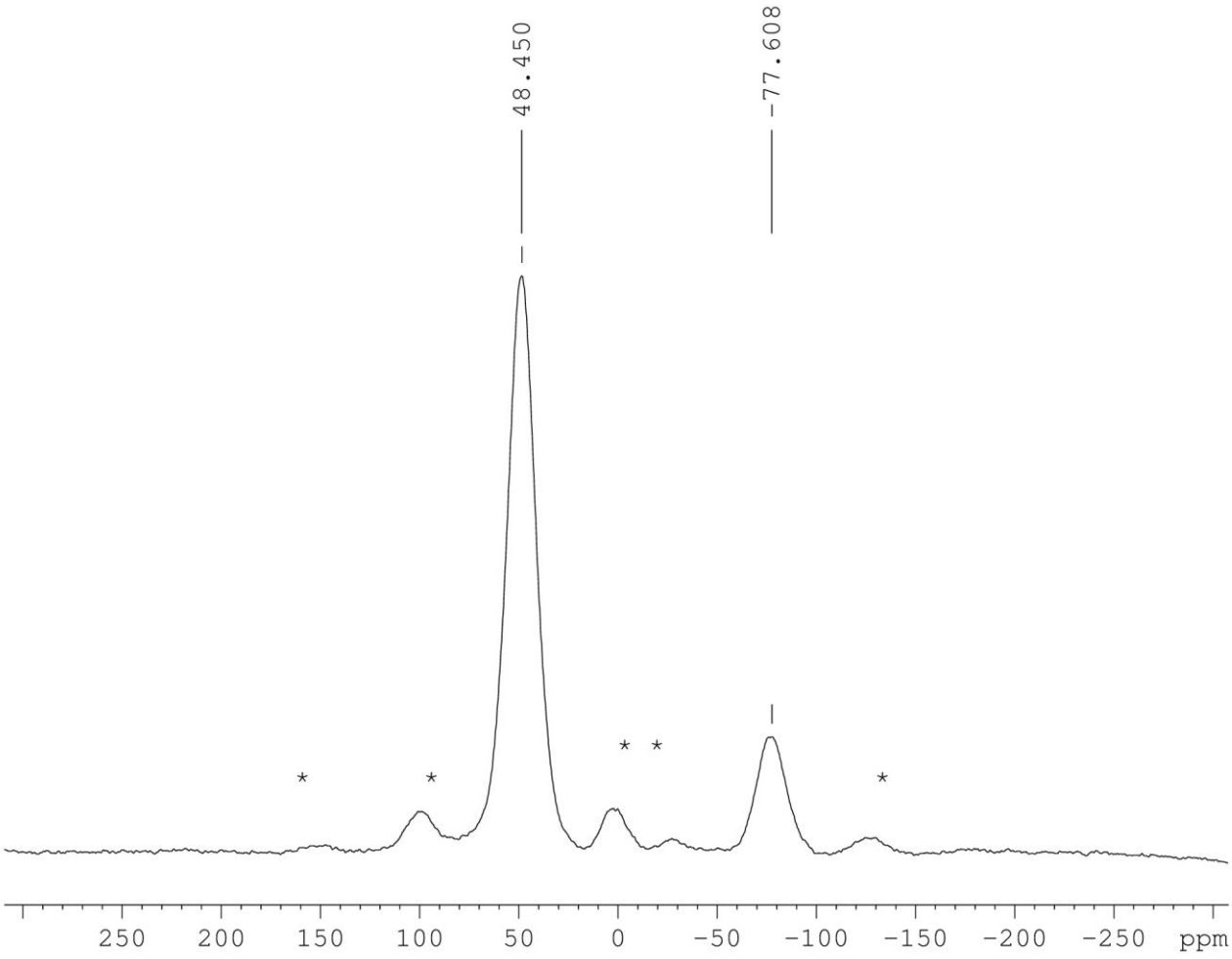

Fig. S13. P-31 CP/MAS spectrum of (**10**)[Cl]$_2$.

NMR detection of [dmePPh][OTf]$_2$, (10)[OTf]$_2$

$PhPCl_2$ (0.180 mg, 1 mmol), dmpe (0.150 g, 1 mmol) and TMSOTf (0.222 g, 2 mmol) were combined in 2 mL CD_3CN and stirred for 5 minutes to yield a clear, colourless solution. The reaction mixture was analyzed by solution PNMR and HNMR.

$^{31}P\{1H\}$ NMR (CD_3CN, 120 MHz, 298 K): -68.4 (*dd*, 275 Hz), 53.9 (*dd*, 277 Hz)

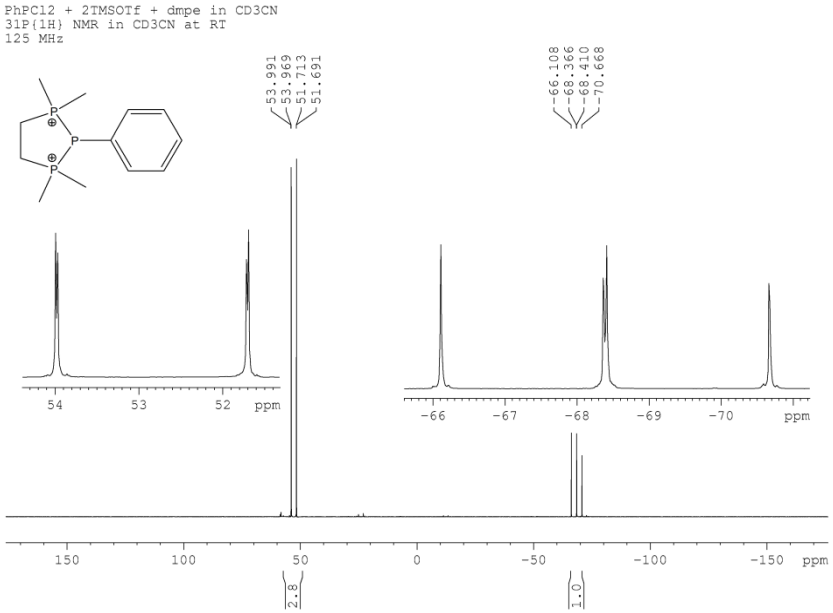

Fig. S14. $^{31}P\{^1H\}$ NMR spectrum of (**10**)[OTf]$_2$ in CD_3CN.

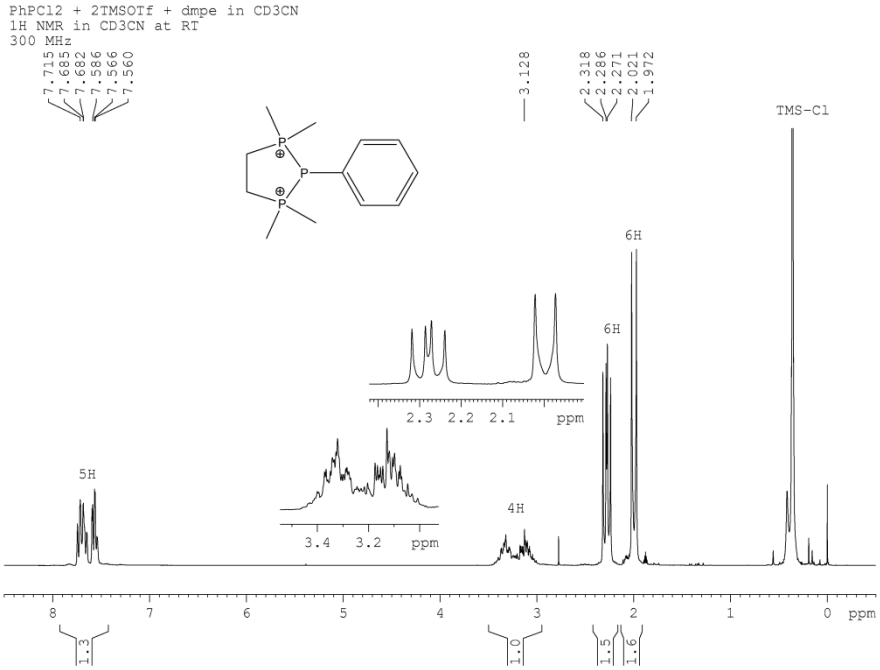

Fig. S15. ^1H NMR spectrum of (**10**)[OTf]$_2$ in CD_3CN.

NMR detection of [$(Me_3P)_2P$][Cl], (**11**)[Cl]

PMe_3 (1.140 g, 15 mmol) was added to PCl_3 (0.686 mg, 5 mmol) in 7 mL dichloromethane to immediately obtain a white precipitate, which became yellow by the end of the addition (1 minute). The reaction mixture was allowed to stir for 1 hour at RT to obtain a yellow suspension. Removal of volatiles yielded a fine yellow powder with some orange flecks (yield = 1.826 g, no loss of material). A small amount of the powder was washed with CD_3CN (low solubility) and analyzed by ^{31}PNMR spectroscopy. The insoluble portion was analyzed by P-31 CP/MAS spectroscopy.

^{31}P{1H} NMR (CD_3CN, 120 MHz, 298 K): -156 (*dd*, 439, 438 Hz), 14.7 (*dd*, 439, 438 Hz)
^{31}P SS NMR (12 kHz): 96 (s, broad, Me_3PCl_2), 26 ppm (broad), 18 (*d*, 436 Hz), -146 (*t*, 432 Hz).

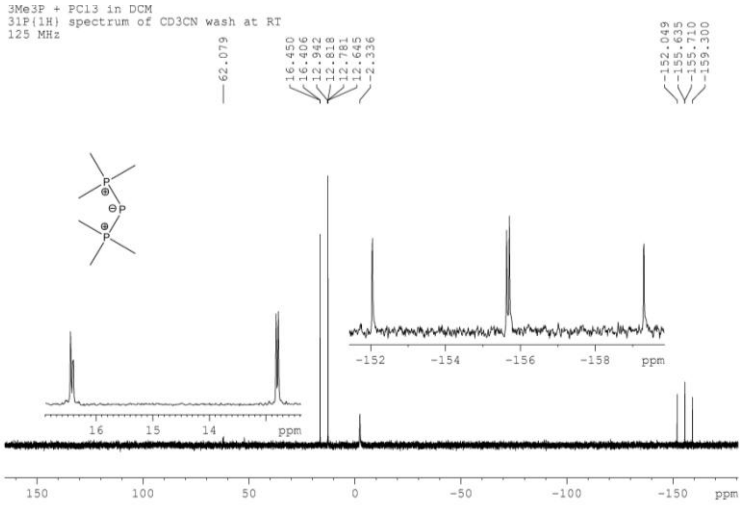

Fig. S16. ^{31}P{^{1}H} NMR spectrum of (**11**)[Cl] in CD_3CN.

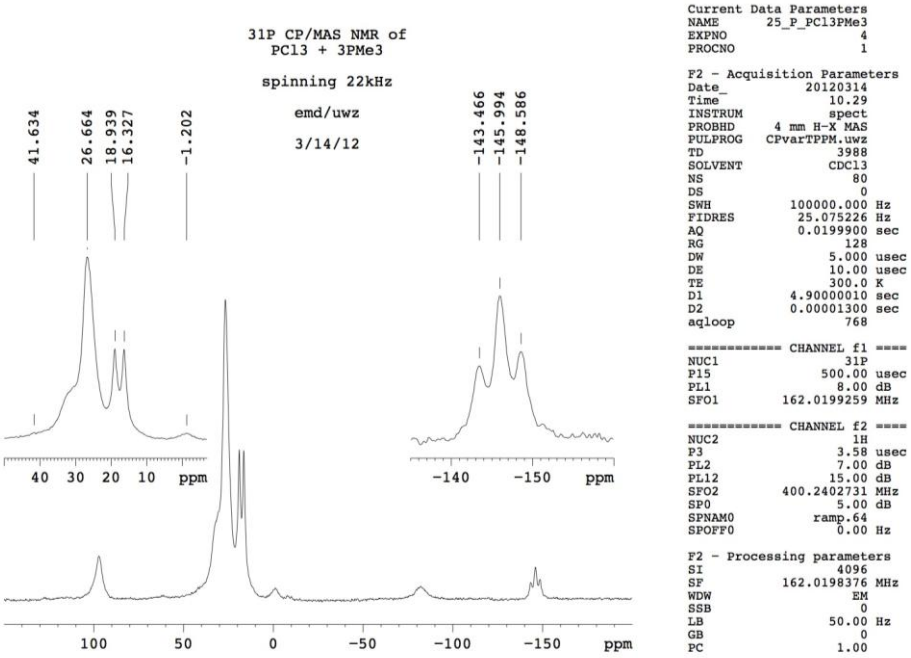

Fig. S17. P-31 CP/MAS spectrum of (**11**)[Cl] and side products Me_3PCl_2 and P*n*.

Attempted synthesis of $[Ph_3PPPh_2][Cl]$

Ph_2PCl (0.221 g, 1 mmol) and Me_3P (0.076 g, 1 mmol) were combined in 1 mL CD_2Cl_2 and stirred for 5 minutes to yield a clear and colourless solution. The ^{31}P NMR spectrum of the one-phase reaction mixture showed no signals in addition to those of the reactants. In a separate experiment, the reagents were combined in fluorobenzene and refluxed overnight. The reaction mixture showed no signals in addition to those of the starting materials.

Attempted synthesis of $[(Ph_3P)_2PMe][Cl]_2$

$MePCl_2$ (0.058 g, 0.5 mmol) and Ph_3P (0.131 g, 0.5 mmol) were combined in 2 mL CD_2Cl_2 and stirred for 5 minutes to yield a clear and colourless solution. The ^{31}P NMR spectrum of the one-phase reaction mixture showed no signals in addition to those of the reactants. In a separate experiment, the reagents were combined in fluorobenzene and refluxed overnight. The reaction mixture showed no signals in addition to those of the starting materials.

Table S2. Optimized Cartesian coordinates for P_2Me_4, $[P_2Me_5]^+$, and $[P_2Me_6]^{2+}$ at the MP2/cc-pVTZ level.

P_2Me_4

P	0.48175	0.99583	0.00000
P	-0.48175	-0.99583	0.00000
C	-0.48175	1.73054	1.40262
C	-0.48175	1.73054	-1.40262
C	0.48175	-1.73054	1.40262
C	0.48175	-1.73054	-1.40262
H	-0.14353	1.30552	2.34627
H	-1.55282	1.56004	1.29496
H	-0.29097	2.80305	1.43396
H	-0.14353	1.30552	-2.34627
H	-0.29097	2.80305	-1.43396
H	-1.55282	1.56004	-1.29496
H	0.14353	-1.30552	-2.34627
H	0.29097	-2.80305	-1.43396
H	1.55282	-1.56004	-1.29496
H	0.14353	-1.30552	2.34627
H	1.55282	-1.56004	1.29496
H	0.29097	-2.80305	1.43396

$[P_2Me_5]^+$

P	0.21819	-0.80639	0.00000
P	-1.00996	1.00700	0.00000
C	-0.20934	1.86776	1.42458
H	0.86557	1.99228	1.31059
H	-0.66648	2.85555	1.48261
H	-0.43495	1.35247	2.35602
C	-0.20934	1.86776	-1.42458
H	0.86557	1.99228	-1.31059
H	-0.43495	1.35247	-2.35602

H	-0.66648	2.85555	-1.48261
C	2.00573	-0.54444	0.00000
H	2.50581	-1.51263	0.00000
H	2.30134	0.00908	-0.88886
H	2.30134	0.00908	0.88886
C	-0.20934	-1.77141	-1.46309
H	0.31955	-2.72304	-1.43594
H	-1.28274	-1.95087	-1.47719
H	0.07796	-1.22849	-2.36138
C	-0.20934	-1.77141	1.46309
H	0.31955	-2.72304	1.43594
H	0.07796	-1.22849	2.36138
H	-1.28274	-1.95087	1.47719

$[P_2Me_6]^{2+}$

P	-0.32786	1.06408	0.00000
P	0.32786	-1.06408	0.00000
C	0.32786	1.84290	1.48258
C	-2.12620	1.08678	0.00000
C	2.12620	-1.08678	0.00000
C	-0.32786	-1.84290	-1.48258
H	-1.41650	-1.81696	-1.48175
H	-0.00138	-2.88519	-1.47373
H	0.06463	-1.36062	-2.37654
H	2.51731	-0.60492	0.89479
H	2.51731	-0.60492	-0.89479
H	2.43805	-2.13357	0.00000
H	-2.51731	0.60492	-0.89479
H	-2.43805	2.13357	0.00000
H	-2.51731	0.60492	0.89479
H	-0.06463	1.36062	2.37654
H	0.00138	2.88519	1.47373
H	1.41650	1.81696	1.48175
C	0.32786	1.84290	-1.48258
H	1.41650	1.81696	-1.48175
H	0.00138	2.88519	-1.47373
H	-0.06463	1.36062	-2.37654
C	-0.32786	-1.84290	1.48258
H	0.06463	-1.36062	2.37654
H	-0.00138	-2.88519	1.47373
H	-1.41650	-1.81696	1.48175

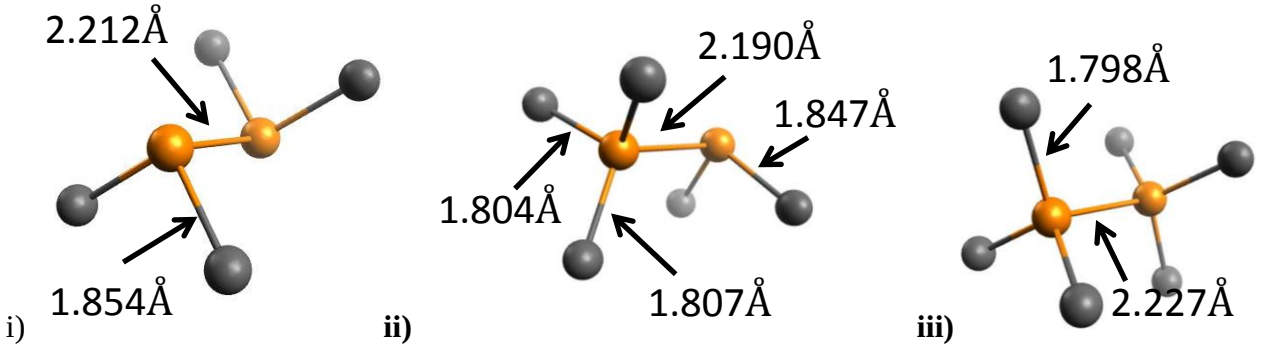

Fig. S18. Optimized structures, P-P and P-C bond lengths for i) P_2Me_4, ii) $[P_2Me_5]^+$, and iii) $[P_2Me_6]^{2+}$

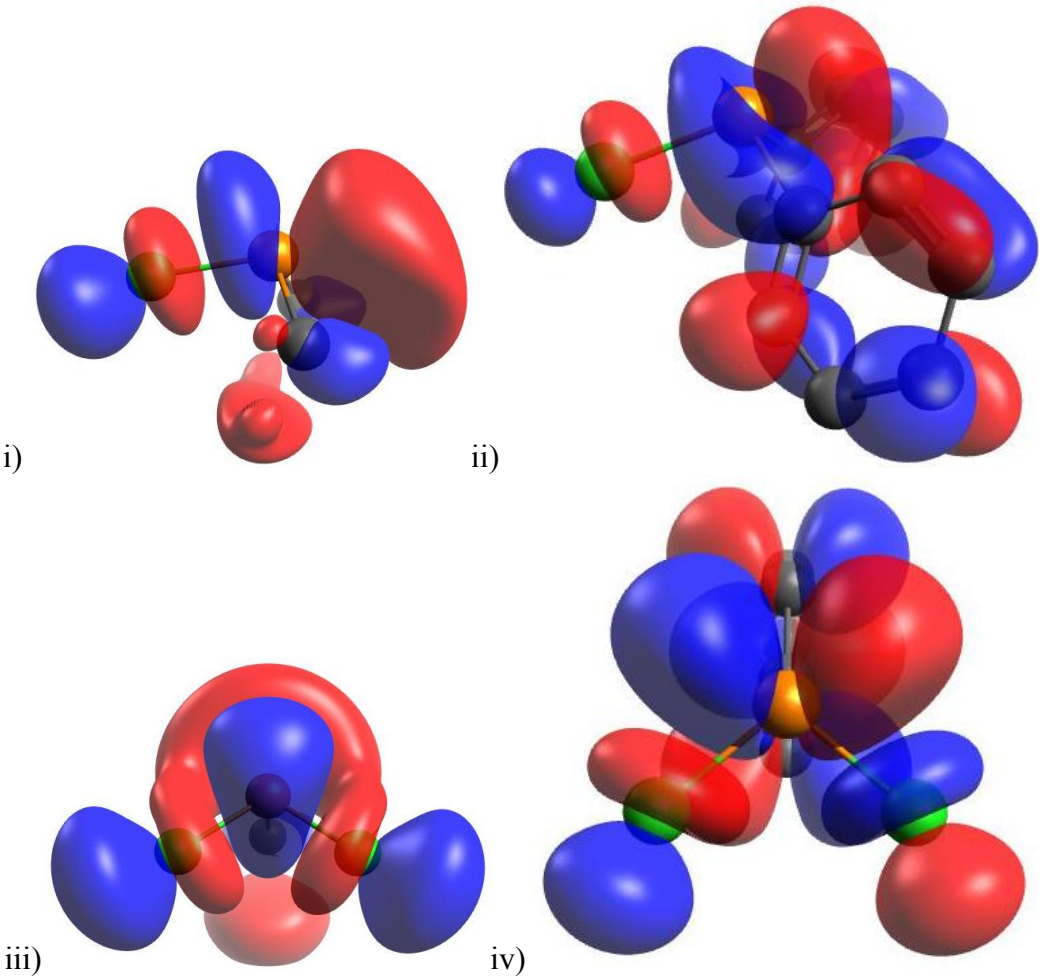

Fig. S19. Pictorial representation of the LUMOs in i) Me_2PCl, ii) Ph_2PCl, iii) $MePCl_2$, and iv) $PhPCl_2$ at the MP2/cc-pVTZ level.

Born-Haber-Fajans cycle for $[Me_3PPMe_2][Cl]$ (all energies in kJ mol^{-1})

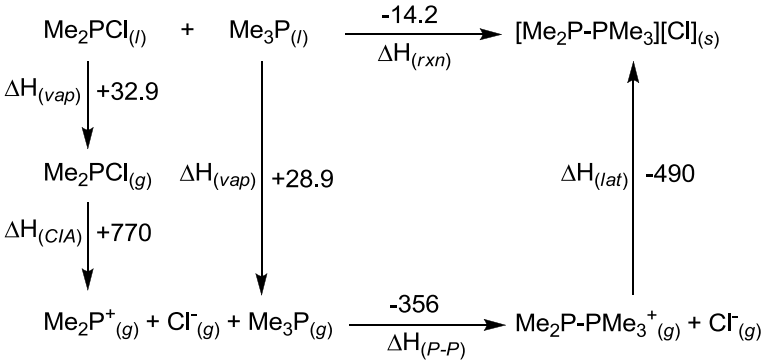

Fig. S20. Born-Haber-Fajans cycle for the synthesis of $[Me_3PPMe_2][Cl]$.

H(vap, Me_2PCl) = +32.9
Ref: Chickos, J. S., and Acree, W. E. Jr., *J. Phys. Chem. Ref. Data*, **2003**, *32*(2), 519.

H(vap, Me_3P) = $H°_f(Me_3P, g) – H°_f(Me_3P, l)$ = +28.9
Ref: Long, L. H., and Sackman, J. F., *Trans. Faraday Soc.*, **1957**, *53*, 1606.

H(CIA) = $H(Me_2P^+, g) + H(Cl^-, g) – H(Me_2PCl, g)$ = +770.3
Gaussian composite G3B3 method using the following reactions:

Rxn 1: $Me_2PCl_{(g)} + AlCl_{3(g)} \rightarrow Me_2P^+_{(g)} + AlCl_4^-{}_{(g)}$ H = +449
Gaussian-09, G3B3 Method

Rxn 2: $AlCl_4 \rightarrow AlCl_{3(g)} + Cl^-_{(g)}$ H = +321
Ref: Pervova, Y. U. *et. al.*, *Russ. J. Phys. Chem.* **1992**, *66*, 635.

Rxn 1 + Rxn 2: $Me_2PCl_{(g)} \rightarrow Me_2P^+_{(g)} + Cl^-_{(g)}$ H = +770

H(P-P) = $H(Me_2P\text{-}PMe_3^+, g) – H(Me_2P^+, g) – H(Me_3P, g)$ = −356.4
Gaussian composite G3B3 method, BSSE-corrected (Counterpoise)

H(lat) = $H([Me_2PPMe_3][Cl], s) − H(Me_2P\text{-}PMe_3^+, g) + H(Cl^-, g)$ = −487
Using Volume Based Thermodynamics.
Ref: Jenkins, H. D. B. and Glasser, L., *J.Chem.Eng.Data*, **2011**, *56*8, 874.

Born-Haber-Fajans cycle for $[Me_3PPMe_2][AlCl_4]$ (all energies in kJ mol^{-1})

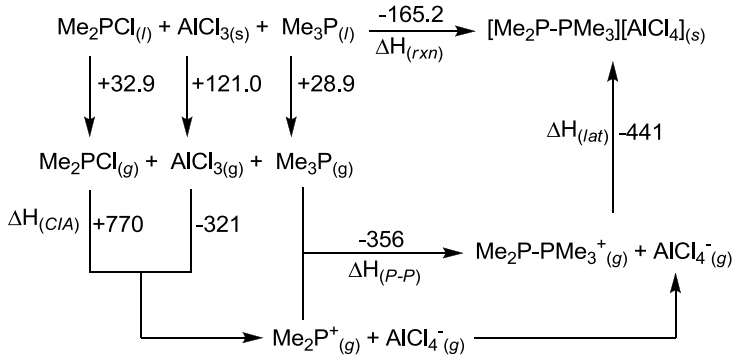

Fig. S21. Born-Haber-Fajans cycle for the synthesis of $[Me_3PPMe_2][AlCl_4]$.

H(sub, $AlCl_3$) = $H°_f(AlCl_3)_{(g)} - H°_f(AlCl_3)_{(s)}$ = +121.0
Ref: Chase, M. W., Jr., *J. Phys. Chem. Ref. Data, Monograph 9*, 1998, 1-1951.

H(lat) = $H([Me_2PPMe_3][AlCl_4], s) - H(Me_2P\text{-}PMe_3^+, g) + H(AlCl_4^-, g)$ = −487
Using Volume Based Thermodynamics.
Ref: Jenkins, H. D. B. and Glasser, L., *J.Chem.Eng.Data*, **2011**, *56*8, 874.
Ref for ionic volume of $AlCl_4^-$: Jenkins, H. D. B., Roobottom, H. K., Passmore, J., and Glasser, L., *Inorg. Chem.*, **1999**, *38*, 3609.
Ionic volume of $P_2Me_5^+$: Molar volume of $[P_2Me_5][Cl]$ (from unit cell) – ionic volume of Cl^- anion = 0.196855 nm^3
Ref for ionic volume of Cl^- : Glasser, L., and Jenkins, H. D. B., *Inorg. Chem.*, **2008**, *47*, 6195.

References

S1. Gaussian 09, Revision A.1, M. J. Frisch, G. W. Trucks, H. B. Schlegel, G. E. Scuseria, M. A. Robb, J. R. Cheeseman, G. Scalmani, V. Barone, B. Mennucci, G. A. Petersson, H. Nakatsuji, M. Caricato, X. Li, H. P. Hratchian, A. F. Izmaylov, J. Bloino, G. Zheng, J. L. Sonnenberg, M. Hada, M. Ehara, K. Toyota, R. Fukuda, J. Hasegawa, M. Ishida, T. Nakajima, Y. Honda, O. Kitao, H. Nakai, T. Vreven, J. A. Montgomery, Jr., J. E. Peralta, F. Ogliaro, M. Bearpark, J. J. Heyd, E. Brothers, K. N. Kudin, V. N. Staroverov, R. Kobayashi, J. Normand, K. Raghavachari, A. Rendell, J. C. Burant, S. S. Iyengar, J. Tomasi, M. Cossi, N. Rega, J. M. Millam, M. Klene, J. E. Knox, J. B. Cross, V. Bakken, C. Adamo, J. Jaramillo, R. Gomperts, R. E. Stratmann, O. Yazyev, A. J. Austin, R. Cammi, C. Pomelli, J. W. Ochterski, R. L. Martin, K. Morokuma, V. G. Zakrzewski, G. A. Voth, P. Salvador, J. J. Dannenberg, S. Dapprich, A. D. Daniels, Ö. Farkas, J. B. Foresman, J. V. Ortiz, J. Cioslowski, and D. J. Fox, Gaussian, Inc., Wallingford CT, 2009.
S2. T. H. Dunning, Jr., *J. Chem. Phys.*, 1989, **90**, 1007.
S3. A. G. Baboul, L. A. Curtiss, P. C. Redfern, and K. Raghavachari, "Gaussian-3 theory using density functional geometries and zero-point energies," *J. Chem. Phys.*, **110**(1999) 7650-57.
S4. S. F. Boys and F. Bernardi, *Mol. Phys.*, 1970, **19**, 553; T. Yanai, D. Tew, and N. Handy, *Chem. Phys. Lett.*, 2004, **393,** 51-57.